

Multi-view Convolutional Neural Networks for 3D Shape Recognition

Hang Su Subhransu Maji Evangelos Kalogerakis Erik Learned-Miller
University of Massachusetts, Amherst
{hsu, smaji, kalo, elm}@cs.umass.edu

Abstract

A longstanding question in computer vision concerns the representation of 3D objects for shape recognition: should 3D objects be represented with shape descriptors operating on their native 3D format, such as their voxel grid or polygon mesh, or can they be effectively represented with view-based descriptors? We address this question in the context of learning to recognize 3D objects from a collection of their rendered views on 2D images. We first present a standard CNN architecture trained to recognize the objects' rendered views independently of each other. Starting from such a network, we show that a 3D object can be recognized even from a single view at an accuracy far higher than using state-of-the-art 3D shape descriptors. The same architecture can be applied to accurately recognize human hand-drawn sketches of objects. Recognition rates further increase when multiple views of the objects are provided. In addition, we present a novel CNN architecture that combines information from multiple views of a 3D object into a single and compact shape descriptor offering even better recognition performance. We conclude that a collection of 2D views can be highly informative for 3D object recognition and is amenable to emerging CNN architectures and their derivatives.

1. Introduction

One of the fundamental challenges of computer vision is to draw inferences about the three-dimensional (3D) world from two-dimensional (2D) images. Since one seldom has access to 3D object models, one must usually learn to recognize and reason about 3D objects based upon their 2D appearances from various viewpoints. Thus, computer vision researchers have typically developed object recognition algorithms from 2D features of 2D images, and used them to classify new 2D pictures of those objects.

But what if one does have access to 3D models of each object of interest? In this case, one can directly train recognition algorithms on 3D features such as voxel occupancy or surface curvature. The possibility of building

such classifiers of 3D shape directly from 3D representations has recently emerged due to the introduction of large 3D shape repositories, such as 3D Warehouse, TurboSquid, and Shapeways. Many authors have produced classifiers of 3D shapes that use 3D representations such as voxel representations directly. For example, when Wu et al. [35] introduced the ModelNet 3D object database, they presented a classifier for 3D shapes using a deep belief network architecture trained on voxel representations.

While intuitively, it seems logical to build 3D shape classifiers directly from 3D models, in this paper we present a surprising and counterintuitive result – that by building classifiers of 3D shapes from 2D image renderings of those shapes, we can actually *dramatically outperform* the classifiers built directly on the 3D representations. In particular, a convolutional neural network (CNN) trained on a fixed set of rendered views of a 3D shape and only provided with a *single* view at test time increases category recognition accuracy by a remarkable 10% (77% \rightarrow 87%) over the best models [35] trained on 3D representations.

One reason for this result is the relative efficiency of the 2D versus the 3D representation. In particular, while a full resolution 3D representation contains all of the information about an object, in order to use a voxel-based representation in a deep network architecture that can be trained with available sample sizes and in a reasonable amount of time, it would appear that the resolution needs to be significantly reduced. For example, 3D ModelNet uses a coarse representation of shape, a $30 \times 30 \times 30$ grid of binary voxels. In contrast a single projection of the 3D model of the same input size corresponds to an image of 164×164 pixels, or slightly smaller if multiple projections are used. Indeed, there is an inherent trade-off between increasing the amount of explicit depth information (3D models) and increasing spatial resolution (projected 2D models).

Another advantage of using 2D representations is that we can leverage (i) advances in image descriptors in the computer vision community [21, 25] and (ii) massive training sets of image data (such as ImageNet [10]) to pre-train our CNN architectures. Because images are ubiquitous and large labeled data sets are abundant, we can learn a good

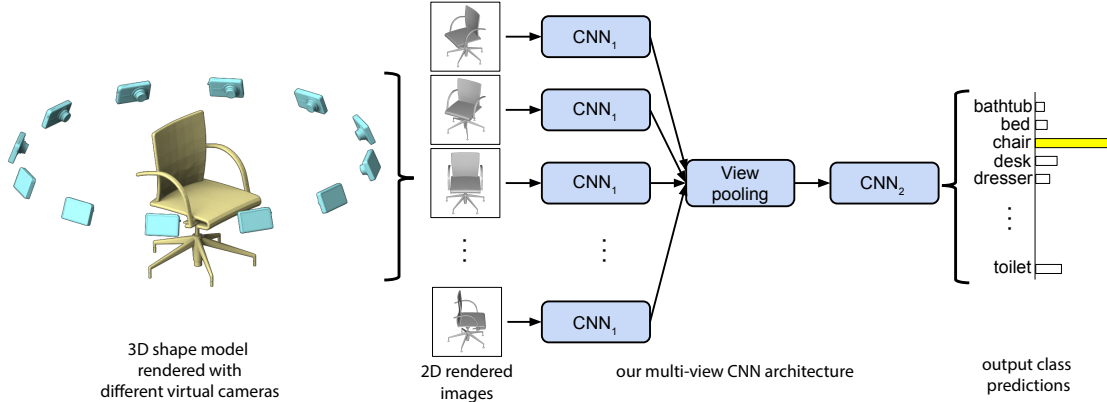


Figure 1. Multi-view CNN for 3D shape recognition. At test time a 3D shape is rendered from 12 different views and are passed through CNN₁ to extract view based features. These are then pooled across views and passed through CNN₂ to obtain a compact shape descriptor.

deal about generic features for 2D image categorization and then fine-tune to specifics about 3D model projections. While it is possible that some day as much 3D training data will be available, for the time being this is a significant advantage of our representation.

Although, the simple strategy of classifying views independently works remarkably well (Section 3.2), we present new ideas for how to “compile” the information in multiple 2D views of an object into a compact descriptor of the object using a new architecture called *multi-view CNN* (Figure 1 and Section 3.3). This descriptor is at least as informative for classification (and for retrieval is slightly more informative) than the full collection of view-based descriptors of the object. Moreover it facilitates efficient retrieval either using a similar 3D object, or retrieval using a simple hand-drawn sketch of a similar object, without resorting to slower methods that are based on pairwise comparison of image descriptors. We present state-of-the-art results on 3D object recognition, 3D object retrieval using 3D objects, and 3D object retrieval using sketches (Section 4).

Our multi-view CNN is related to “jittering” where transformed copies of the data are added during training to learn invariances to transformations such as rotation or translation. In the context of 3D recognition the views can be seen as jittered copies. The multi-view CNN learns to combine the views instead of averaging, and thus can use the more informative views of the object for prediction while ignoring others. Our experiments show that this improves performance (Section 4.1) and also lets us visualize informative views of the object by back-propagating the gradients of the network to the views (Figure 3). Even on traditional image classification tasks multi-view CNN can be a better alternative to jittering. For example on the sketch recognition benchmark [12] jittered copies of a training example combined with a multi-view CNN performs better than a standard CNN training with jittered copies (Section 4.2). This also advances the state-of-the-art from 79.0% [29] to 87.2% approaching human performance on this task.

2. Related Work

Our method is related to prior work on shape descriptors for 3D objects and image-based CNNs. Next we discuss the most representative works in these areas.

Shape descriptors. A large corpus of shape descriptors has been developed for drawing inferences about 3D objects in both the computer vision and graphics literature. Shape descriptors can be classified into two broad categories: *3D shape descriptors* that directly work on the native 3D representations of objects, such as polygon meshes, voxel-based discretizations, point clouds, or implicit surfaces, and *view-based descriptors* that describe the shape of a 3D object by “how it looks” in a collection of 2D projections.

With the exception of the recent work of Wu et al. [35] which learns shape descriptors from the voxel-based representation of an object through 3D convolutional nets, previous descriptors were largely “hand-designed” according to a particular geometric property of the shape surface or volume. For example, shapes can be represented with histograms or bags-of-features models constructed out of surface normals and curvatures [16], distances, angles, triangle areas or tetrahedra volumes gathered at randomly sampled surface points [24], properties of spherical functions defined in volumetric grids [17], local shape diameters measured at densely sampled surface points [5], heat kernel signatures on polygon meshes [2, 3], or extensions of the SIFT and SURF feature descriptors to 3D voxel grids [18]. Developing classifiers and other supervised machine learning algorithms on top of such 3D shape descriptors poses a number of challenges. First, the size of organized databases with annotated 3D models is rather limited compared to image datasets e.g. ModelNet contains about 150K shapes (its 40 category benchmark contains about 10K shapes). In contrast, the ImageNet dataset [10] already includes tens of millions of annotated images.

On the other hand view-based descriptors have a num-

ber of desirable properties: they are low-dimensional, efficient to evaluate, and robust to 3D shape representation artifacts, such as holes, imperfect polygon mesh tessellations, noisy surfaces. The rendered shape views can also be directly compared with other 2D images, silhouettes or even human sketches. An early example of a view-based approach is the work by Murase and Nayar [23] that recognizes objects by matching their appearance in parametric eigenspaces formed by large sets of 2D renderings of 3D models under varying poses and illuminations. Another example, which is particular popular in computer graphics setups, is the LightField descriptor [6] that extracts a set of geometric and Fourier descriptors from object silhouettes rendered from several different viewpoints. Alternatively, the silhouette of an object can be decomposed into parts and then be represented by a directed acyclic graph (shock graph) [22]. Cyr and Kimia [9] define similarity metrics based on curve matching and grouped similar views, called aspect graphs of 3D models [19]. Eitz et al. [13] compare human sketches with line drawings of 3D models produced from several different views based on local Gabor filters, while Schneider et al. [29] propose Fisher Vectors [25] on SIFT features [21] for representing human line drawings of objects. Existing view-based descriptors are largely “hand-engineered” and some do not generalize well across different domains e.g., the Lightfield descriptor requires closed silhouettes and cannot be applied to sketches.

Convolutional neural networks. Our work is also related to recent advances in image recognition using deep CNNs [20]. In particular CNNs trained on the large datasets such as ImageNet have been shown to learn general purpose image descriptors for a number of recognition tasks such as object detection, scene recognition, texture recognition and fine-grained classification [11, 14, 27, 8]. We show that these deep architectures can be adapted to specific domains including shaded illustrations of 3D objects, line drawings, and human sketches to produce descriptors that have dramatically superior performance compared to other view-based descriptors and 3D shape descriptors (including 3D ShapeNets [35]) in a variety of setups: shape retrieval, classification and sketch recognition. Furthermore, they are compact and efficient to compute.

Although, there is significant work on 3D and 2D shape descriptors, and estimating informative views of the objects (or, aspect graphs), there is relatively little work on learning to combine the view-based descriptors for 3D model recognition. Most methods resort to simple strategies such as performing exhaustive pairwise comparisons of descriptors extracted from different views of each model. In contrast our multi-view CNN architecture learns to recognize 3D shapes from views of objects using image-based CNNs but in the *context* of other views via a view-pooling layer. As a result,

information from multiple views is effectively accumulated into a single, compact shape descriptor.

3. Method

As discussed above, our focus in this paper is on developing view-based descriptors of 3D objects that are trainable, produce informative representations for recognition and retrieval tasks, and are efficient to produce.

Our view-based representations start from multiple views of a 3D object, generated by a rendering engine. A simple way to use multiple views is to generate a 2D image descriptor per each view, and then use the individual descriptors directly for recognition tasks based on some voting scheme. For example, a naïve approach would be to average the individual descriptors, treating all the views as equally important. Alternatively, if the views were rendered in a reproducible order, one could also concatenate the representations of each view. Unfortunately, aligning a 3D model to a canonical orientation is hard and sometimes ill-defined. In contrast to the above simple approaches, an aggregated representation combining features from multiple views is more desirable since it yields a single, compact descriptor representing the 3D object.

Our approach is to learn to combine information from multiple views using a unified CNN architecture that includes a view-pooling layer (Figure 1). All the parameters of our CNN architecture are learned discriminatively to produce a single compact descriptor for the 3D object. Compared to exhaustive pairwise comparisons between different single-view representations of 3D shapes, our resulting descriptor can be directly used to compare 3D shapes leading to significantly higher computational efficiency.

3.1. Input: A multi-view representation

3D models in online databases are typically stored as polygon meshes, which are collections of points connected with edges forming faces. We assume that the 3D models are consistently upright oriented. Most models in modern online repositories, such as the 3D Warehouse, satisfy this requirement. For each mesh, we render 12 projected views as follows: we place 12 different virtual cameras (viewpoints) around it every 30 degrees (see Figure 1). The cameras are elevated 30 degrees from the ground plane, pointing towards the centroid of the models. The centroid is calculated as the weighted average of the mesh face centers, where the weights are the face areas. The shapes are illuminated using the Phong reflection model [26]: each mesh vertex is assigned with a reflected grayscale light intensity according to an ambient term simulating light coming from all directions, and a diffuse (Lambertian) term simulating a point light placed at each viewpoint. For each vertex v with unit normal vector \mathbf{n} and a unit light vector \mathbf{l} estimated as the direction vector from the vertex towards a

viewpoint, the reflected intensity at the vertex is calculated as: $I_v = k_a + k_d \cdot \max(\mathbf{l} \cdot \mathbf{n}, 0)$, where k_a, k_d are the ambient and diffuse term coefficients set to 0.1 and 0.9 respectively in our implementation. The mesh polygons are rendered under a perspective projection and the pixel color is determined by interpolating the reflected intensity of the polygon vertices. Shapes are uniformly scaled to fit into the viewing volume. We note that using different shading coefficients or illumination models did not affect our output descriptors due to the invariance of the learned filters to illumination changes, as also observed in image-based CNNs [20, 11]. Adding more or different viewpoints is trivial, however, we found that the above camera setup was enough to already achieve high performance. Finally, rendering each mesh from all the viewpoints takes no more than ten milliseconds on modern graphics hardware.

3.2. Recognition with multi-view representation

We claim that our multi-view representation contains rich information about 3D shapes and can be applied for various types of tasks related to 3D shapes. In the first setting, we make use of existing 2D image features directly and produce a descriptor for each view. This is the most straightforward approach to utilize multi-view representations for 3D shapes, and has the obvious benefit that image representation has been a very active and fruitful research area and many robust image features exist. This however results in multiple 2D image descriptors per 3D shape, one per view, which need to be integrated for recognition tasks.

Image descriptors. We use two types of image descriptors for each 2D image: a state-of-the-art “hand-crafted” image descriptor based on Fisher vectors [28] with multi-scale SIFT, as well as CNN activation features [11].

The Fisher vector feature is implemented using VLFEAT [34]. For each image multi-scale SIFT descriptors are extracted densely. These are then PCA projected to 80 dimensions followed by Fisher vector pooling with a Gaussian mixture model with 64 components, square-root and ℓ_2 normalization.

For our CNN features we use the VGG-M network from [4] which consists of five convolutional ($\text{conv}_{1,\dots,5}$) and pooling layers followed by two fully connected layers $\text{fc}_{6,7}$ and classification layer. The network is pre-trained on ImageNet images from 1k categories, and then fine-tuned on all 2D views of the 3D shapes in training set. As we show in our experiments, fine-tuning improves performance significantly. Both Fisher vectors and CNN features yield very good performance in classification and retrieval compared with popular 3D shape descriptors (e.g. SPH [17], LFD [6]) as well as 3D ShapeNets [35].

Classification. We train one-vs-all linear SVMs (each view as separate training samples) to classify shapes with view-based image features. At test time, we simply sum up SVM decision values over all 12 views and return the class with the highest total. Alternative approaches, e.g. averaging image descriptors, lead to worse accuracy in our experiments.

Retrieval. A distance or similarity measure is required for retrieval tasks. For shape \mathbf{x} with n_x image descriptors and shape \mathbf{y} with n_y image descriptors, distance between them is defined in Eq. 1. Here distance between 2D images is defined as L2 distance between their feature vectors, e.g. $\|\mathbf{x}_i - \mathbf{y}_j\|_2$.

$$Dist(\mathbf{x}, \mathbf{y}) = \frac{1}{2} \frac{\sum_j \min_i \|\mathbf{x}_i - \mathbf{y}_j\|_2}{n_y} + \frac{1}{2} \frac{\sum_i \min_j \|\mathbf{x}_i - \mathbf{y}_j\|_2}{n_x} \quad (1)$$

To interpret this definition, we can first define the distance between a 2D image \mathbf{x}_i and a 3D shape \mathbf{y} as $d(\mathbf{x}_i, \mathbf{y}) = \min_j \|\mathbf{x}_i - \mathbf{y}_j\|_2$. Then given all n_x distances between \mathbf{x} ’s 2D projections and \mathbf{y} , the distance between these two shapes can be get by simple averaging. In Eq. 1, this idea is applied in both directions to ensure distance symmetry.

In our experiments we analyzed alternative distances measures, such as minimum distances among all $n_x \cdot n_y$ image pairs, distance between average image descriptors, but they all lead to inferior performance.

3.3. Multi-view CNN: Learning to aggregate views

Although very successful for classification and retrieval compared with existing 3D descriptors, having multiple separate descriptors for each 3D shape can be inconvenient and inefficient in many cases. For example, in Eq. 1, we need to compute all $n_x \cdot n_y$ pairwise distances between image pairs in order to compute distance between two 3D shapes. Simply averaging or concatenating the image descriptors leads to inferior performance. In this section, we take aim at the problem of learning to aggregate multiple views in order to synthesize the information from all views into a single, compact 3D shape descriptor.

We design the Multi-view CNN (MVCNN) based on a standard 2D image CNN with linear structure. Each image in a 3D shape’s multi-view representation is passed through the first part of the network (CNN_1) separately, and aggregated using element-wise maximum before sent through the remaining part of the network CNN_2 (see Figure 1). All branches in the first part of the network (CNN_1) share the same parameters. MVCNN are directed acyclic graphs and

can be trained or fine-tuned using stochastic gradient descent with back-propagation with mini-batches. The view-pooling layer is closely related to max-pooling layer and maxout layer [15], with the only difference being the dimension their the pooling operations are carried on.

View-pooling layer can be placed anywhere in the network. We show in our experiments that it is best to place it after one of the fully connected layers (fc_6 , fc_7 , etc.). Also an alternative is to use element-wise mean instead of element-wise maximum in the view-pooling layer, but it is not as effective in terms of classification and retrieval performance in our experiments.

Our aggregated shape descriptor yields higher performance than using separate image descriptors directly, especially in retrieval (73.04% vs. 68.72%). And perhaps more importantly, the aggregated descriptor is ready for use out of the box for various 3D tasks, e.g. 3D shape classification and retrieval, and offers significant speed-ups against multiple image descriptors.

MVCNN can also be used as a general framework to integrate perturbed image samples (also known as data jittering). We illustrate its capability in the context of sketch recognition in Section 4.2.

4. Experiments

4.1. 3D shape classification and retrieval

We evaluate our shape representations on the Princeton ModelNet dataset [1]. ModelNet currently contains 127,915 3D CAD models from 662 categories¹. A 40-class well-annotated subset containing 12,311 shapes from 40 common categories, ModelNet40, is provided with standard training and testing splits on the ModelNet website.²

Our shape representations are compared against the 3D ShapeNet descriptors by Wu *et al.* [35], the Spherical Harmonics descriptor (SPH) by Kazhdan *et al.* [17], the Light-Field descriptor (LFD) by Chen *et al.* [6], and Fisher vectors extracted on the same rendered views of the shapes used as input to our network.

The comparisons on shape classification and retrieval is summarized in Table 1. Precision-recall curves are provided in Figure 2. Remarkably the Fisher vector baseline with just a single view achieves a classification accuracy of 79.59% outperforming the state-of-the-art learned 3D descriptors (77.32% [35]). When all 12 views of the shape are available at test time, we can also average the predictions over these views. Averaging increases the performance of

¹As of 04/21/2015.

²We note that Wu *et al.* [35] switched to a smaller subset of ModelNet40 containing only 4,000 shapes in the camera-ready version. Evaluation with the full ModelNet40 can still be found in the supplementary material available on the ModelNet website. The exact new training/test split however is not publicly available as of this date. Thus, we experiment with the full ModelNet40 and evaluate all the methods on this set.

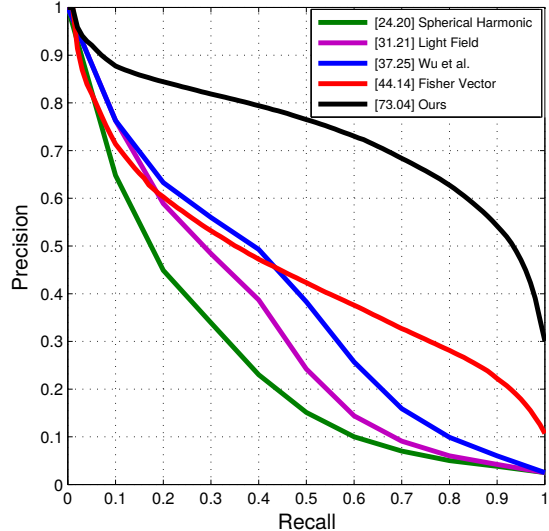


Figure 2. Precision-recall curves for various methods for 3D shape retrieval on the ModelNet40 dataset. Our method significantly outperforms the state-of-the-art on this task achieving 73.04% mAP.

Fisher vectors to 84.82%. The performance of Fisher vectors further supports our claim that 3D objects can be effectively represented using view-based 2D representations. The trends for shape retrieval are also similar.

Using our CNN baseline [4] trained on ImageNet in turn outperforms Fisher vectors by a significant margin. Fine-tuning the CNN on the rendered views of the training shapes of ModelNet40 further improves the performance. By using all 12 views of the shape, its classification accuracy reaches 90.24%. The retrieval accuracy is also improved to 68.72%.

Our multi-view CNN outperforms all the state-of-the-art descriptors as well as the Fisher vector and view-based CNN baselines. With fine-tuning on the ModelNet40 training split, our model achieves 90.92% classification accuracy, and 73.04% mean average precision (mAP) on retrieval. The performance gains over the view-based CNN baselines are particularly significant on the retrieval task, which suggests the important role of aggregating the view based descriptors. Our multi-view CNN constitutes an absolute gain of 13.5% in classification accuracy compared to the state-of-the-art learned 3D shape descriptors [35] (77.32% \rightarrow 90.92%). Similarly, retrieval accuracy is improved by 35.8% (37.25 \rightarrow 72.04%).

We also consider different locations to place the view-pooling layer in our multi-view CNN architecture. In our experiments (Table 2), fc_7 is the best layer to perform view-pooling for classification, while fc_6 is a slightly better choice for retrieval.

Saliency map among views. For each 3D shape S , our multi-view representation consists of a set of K 2D views

Method	Training Config.			Test Config.	Classification (Accuracy)	Retrieval (mAP)
	Pre-train	Fine-tune	#Views	#Views		
(1) SPH [17]	-	-	-	-	63.59%	24.20%
(2) LFD [6]	-	-	-	-	75.47%	31.21%
(3) 3D ShapeNets [35]	ModelNet40	ModelNet40	-	-	77.32%	37.25%
(4) FV	-	ModelNet40	12	1	79.59%	37.82%
(5) FV, 12×	-	ModelNet40	12	12	84.82%	44.14%
(6) CNN	ImageNet1K	-	-	1	85.47%	42.63%
(7) CNN, fine-tuned	ImageNet1K	ModelNet40	12	1	87.04%	66.26%
(8) CNN, 12×	ImageNet1K	-	-	12	89.95%	49.61%
(9) CNN, fine-tuned, 12×	ImageNet1K	ModelNet40	12	12	90.24%	68.72%
(10) MVCNN, 12×	ImageNet1K	-	-	12	90.32%	50.80%
(11) MVCNN, fine-tuned, 12×	ImageNet1K	ModelNet40	12	12	90.92%	73.04%

Table 1. Classification and retrieval results on the ModelNet40 dataset. On the top are results using state-of-the-art 3D shape descriptors. Our view-based descriptors including Fisher vectors (FV) significantly outperform these even when a single view is available at test time (#Views = 1). When multiple views (#Views=12) are available at test time, the performance of view-based methods improve significantly. The multi-view CNN (MVCNN) architecture outperforms the view-based methods, especially for retrieval. Fine-tuning helps in all cases.

Layer	Classification (Accuracy)	Retrieval (mAP)
conv ₃	89.42%	66.60%
conv ₄	89.95%	69.32%
conv ₅	89.99%	72.18%
fc ₆	90.36%	74.72%
fc ₇	90.92%	73.04%

Table 2. Comparison of various view-pooling locations in the multi-view CNN architecture.

$\{I_1, I_2 \dots I_K\}$. We would like to rank pixels in the 2D views w.r.t. their influence on the output score F_c of the network (e.g. taken from fc₈ layer) for its ground truth class c . Following [31], saliency maps can thus be defined as the derivatives of F_c w.r.t. the 2D views of the shape:

$$[w_1, w_2 \dots w_K] = \left[\frac{\partial F_c}{\partial I_1} \Big|_S, \frac{\partial F_c}{\partial I_2} \Big|_S, \dots, \frac{\partial F_c}{\partial I_K} \Big|_S \right] \quad (2)$$

For MVCNN, w in Eq. 2 can be computed using back-propagation with all the network parameters fixed, and can then be rearranged into saliency maps for individual views. Examples of saliency maps are shown in Figure 3.

4.2. Sketch recognition: jittering revisited

Given the success of our aggregated representation on multiple views of a 3D object, it is logical to ask whether aggregating multiple views of a two-dimensional image could also improve performance. Here we show that this is indeed

the case by exploring its connection with data jittering in the context of sketch recognition.

Data jittering (also known as data augmentation) is a method to generate extra samples from a given image. It is the process of perturbing the image by transformations that change its appearance while leaving the high-level information (class label, attributes, *etc.*) intact. Jittering can be applied at training time to augment training samples and to reduce overfitting, or at test time to provide more robust predictions. In particular, several authors [20, 4, 33] have used data jittering to improve the performance of deep representations on two-dimensional image classification tasks. In these applications, jittering at training time usually includes random images translations (implemented as random crops), horizontal reflections, and color perturbing. At test time jittering usually only includes a few crops (for example, four at the corners, one at the center and their horizontal reflections). We now examine whether we can get more benefit out of jittered views of an image by using the same feature aggregation scheme we developed for recognizing 3D shapes.

The human sketch dataset [12] contains 20,000 hand-drawn images of 250 object categories such as airplanes, apples, bridges, *etc.* The accuracy of humans in recognizing these hand-drawings is only 73% for a number of reasons including the quality of the sketches drawn. In a subsequent paper [29], Schneider and Tuytelaars cleaned up the data by removing instances that humans find hard to recognize, and keeping only categories that have at least 56 images. This filtered dataset (SketchClean) contains 160 categories, on which human can achieve 93% recognition accuracy. The current state-of-the-art on sketch recognition is 67.6% ac-

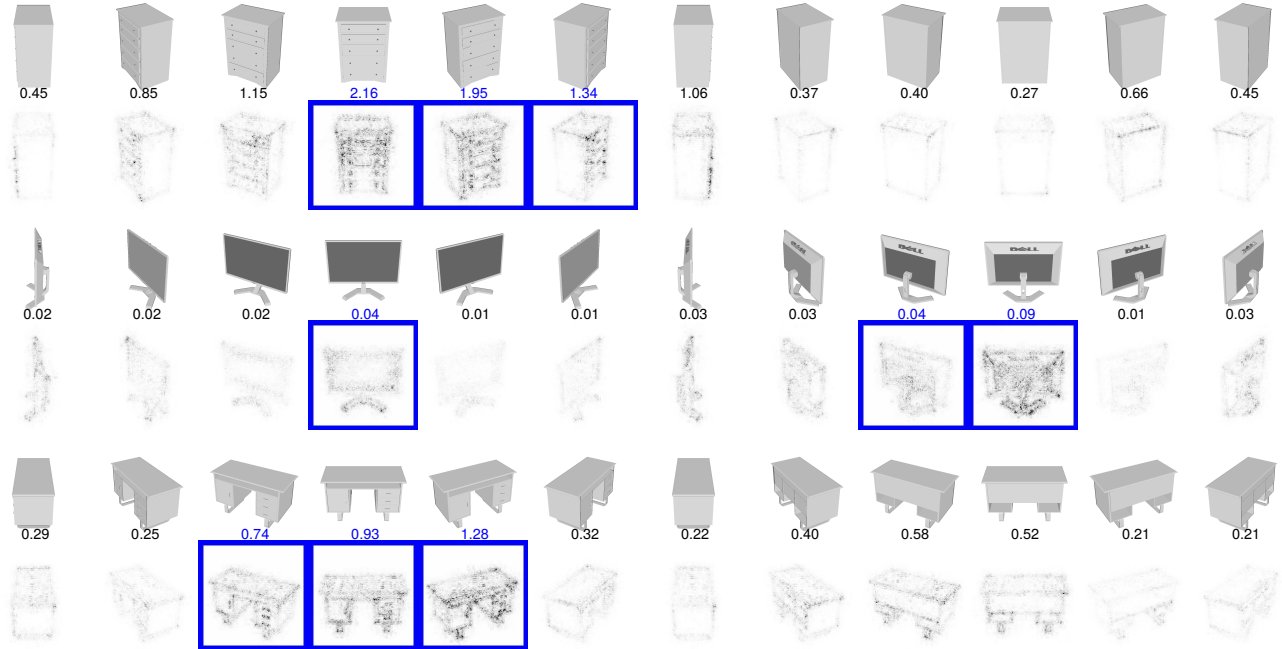


Figure 3. Top three views with the highest saliency are highlighted in blue and the relative magnitudes of gradient energy for each view is shown on top. The saliency maps are computed by back-propagating the gradients of the class score onto the image via the view-pooling layer. Notice that the handles of the dresser and of the desk are the most discriminative features. (Figures are enhanced for visibility).

accuracy on the original sketch dataset and 79.0% accuracy on the SketchClean dataset, achieved by using SIFT Fisher vectors with spatial pyramid pooling and linear SVMs [29]. We split the SketchClean dataset randomly into training, validation and test set³, and report classification accuracy on the test set in Table 3.

With an off-the-shelf CNN (VGG-M from [4]), we are able to get 77.3% classification accuracy without any network fine-tuning. With fine-tuning on the training set, the accuracy can be further improved to 84.0%, significantly surpassing the Fisher vector approach. These numbers are achieved by using the penultimate layer (fc_7) in the network as image descriptors and linear SVMs.

Although it is impracticable to get multiple views from 2D images, we can use jittering to mimic the effect of views. For each hand-drawing, we do in-plane rotation with three angles: -45° , 0° , 45° , and also their horizontal reflections (hence 6 samples per image). We apply the two CNN variants (with and without the view-pooling layer) discussed earlier for aggregating multiple views of 3D shapes, and get 85.5% (fine-tuned w/o view-pooling layer) and 86.3% (fine-tuned w/ view-pooling layer) classification accuracy respectively. The latter also has the advantage of a single, more compact descriptor for each human sketch.

With a deeper network architecture (VGG-VD, which is a network with 16 weight layers from [32]), we are able to

³The dataset does not come with a standard training/val/test split.

Method	Aug.	Accuracy
(1) FV [29]	-	79.0%
(2) CNN M	-	77.3%
(3) CNN M, fine-tuned	-	84.0%
(4) CNN M, fine-tuned	6×	85.5%
(5) MVCNN M, fine-tuned	6×	86.3%
(6) CNN VD	-	69.3%
(7) CNN VD, fine-tuned	-	86.3%
(8) CNN VD, fine-tuned	6×	86.0%
(9) MVCNN VD, fine-tuned	6×	87.2%
(10) Human performance	n/a	93.0%

Table 3. Sketch classification results. Fine-tuned CNN models significantly outperform the state-of-the-art by a significant margin. Multi-view CNNs are better than CNN training with data jittering. The results are shown with two different CNN architectures – VGG-M (row 2-5) and VGG-VD (row 6-9).

achieve 87.2% accuracy, advancing the state of the art by a large margin, and closely approaching human performance.

4.3. Sketch-based 3D shape retrieval

Due to the growing number of online 3D shape repositories, a number of different approaches have been investigated to perform efficient 3D shape retrieval. Several online

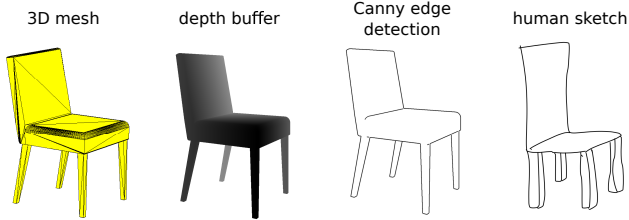


Figure 4. Line-drawing style rendering from 3D shapes.

repositories (e.g. 3D Warehouse, TurboSquid, Shapeways) support only text-based search engines or hierarchical catalogs for 3D shape retrieval. However, it is hard to convey stylistic and geometric variations using only textual descriptions, thus sketch-based shape retrieval [36, 30, 13] has been proposed as an alternative for users to retrieve shapes with an approximate line-drawing of the desired 3D shape in mind. Sketch-based retrieval is challenging since it involves two heterogeneous data domains (hand-drawn sketches and 3D models). Sketches can be highly abstract and visually different from target 3D shapes. Here we demonstrate the potential strength of our multi-view CNN in sketch-based shape retrieval.

For this experiment, we construct a dataset containing 193 sketches and 790 CAD models from 10 categories existing in both SketchClean and ModelNet40. Following [13], we produce renderings of 3D shapes with a style similar to hand-drawn sketches (see Figure 4). This is achieved by detecting Canny edges on the depth buffer (also known as z -buffer) of the 3D mesh renderings from 12 viewpoints, as described in Section 3.1. These views are passed through the view-based CNN to obtain a image descriptor. For a query sketch image, we use the multi-view CNN descriptor described in Section 4.2 pooled from 6 perturbed samples per query. Several strategies are possible, but in this experiment we match the sketch descriptor to the 3D shape using the “average minimum distance” (Equation 1) to its view descriptors. Representative retrieval results are shown in Figure 5 with false matches highlighted in red.

We are able to retrieve 3D objects that share the class label with the query sketch, as well as being visually similar, especially in the top few matches. Our performance is 36.08% mAP on this dataset. We note that we use here the VGG-M network trained on ImageNet dataset without any fine-tuning on either sketches or 3D shapes. With a fine-tuning procedure that optimizes a distance measure between hand-drawn sketches and 3D shapes, e.g. by using a Siamese Network [7], retrieval performance can be further improved.

5. Conclusion

While the world is full of 3D shapes, as humans at least, we understand that world mostly through 2D images. We

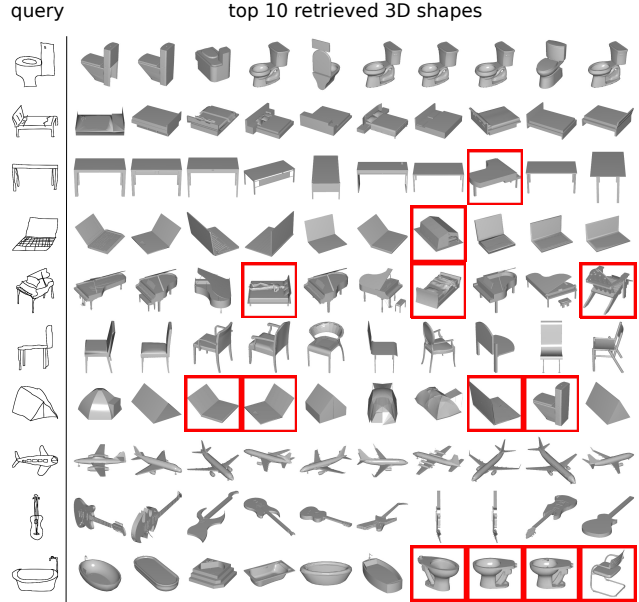


Figure 5. Sketch-based 3D shape retrieval examples. For each query we show the top 3D shapes that match the query. Mistakes are highlighted in red.

have shown that using images of shapes as inputs to modern learning architectures, we can achieve performance better than any previously published results, including those that operate on direct 3D representations of shape.

While even a naive usage of these multiple 2D projections yields impressive classification and discrimination performance, we have shown that by building descriptors that are aggregations of information from multiple 2D views, we can achieve compactness, efficiency, and high accuracy using a single descriptor. In addition, by relating the content of 3D models to 2D representations like sketches, we can retrieve these 3D models at high accuracy rates by using the sketches, and leverage the implicit knowledge of 3D shape contained in these 2D views.

There are a number of directions to explore in future work. One is to experiment with different combinations of 2D views. Which views are most informative? How many views are necessary for a given level of accuracy? Can informative views be selected on the fly?

In addition, our techniques can be applied to real objects rather than merely 3D polygonal shape models. An obvious question is whether our view aggregating descriptors can be used for building compact and discriminative descriptors for real-world 3D objects from multiple views, or automatically from video. Such investigations could be immediately applicable to widely studied problems such as object recognition and face recognition.

- [18] J. Knopp, M. Prasad, G. Willems, R. Timofte, and L. Van Gool. Hough transform and 3d surf for robust three dimensional classification. In *Proc. ECCV*, 2010. 2
- [19] J. J. Koenderink and A. J. Van Doorn. The singularities of the visual mapping. *Biological cybernetics*, 24(1):51–59, 1976. 3
- [20] A. Krizhevsky, I. Sutskever, and G. E. Hinton. Imagenet classification with deep convolutional neural networks. In *Proc. NIPS*. 2012. 3, 4, 6
- [21] D. G. Lowe. Object recognition from local scale-invariant features. In *Proc. ICCV*, 1999. 1, 3
- [22] D. Macrini, A. Shokoufandeh, S. Dickinson, K. Siddiqi, and S. Zucker. View-based 3-d object recognition using shock graphs. In *Proc. ICPR*, volume 3, 2002. 3
- [23] H. Murase and S. K. Nayar. Visual learning and recognition of 3-d objects from appearance. 14(1), 1995. 3
- [24] R. Osada, T. Funkhouser, B. Chazelle, and D. Dobkin. Shape distributions. *ACM Trans. Graph.*, 21, 2002. 2
- [25] F. Perronnin, J. Sánchez, and T. Mensink. Improving the Fisher kernel for large-scale image classification. In *Proc. ECCV*, 2010. 1, 3
- [26] B. T. Phong. Illumination for computer generated pictures. *Commun. ACM*, 18(6), 1975. 3
- [27] A. S. Razavin, H. Azizpour, J. Sullivan, and S. Carlsson. Cnn features off-the-shelf: An astounding baseline for recognition. In *DeepVision workshop*, 2014. 3
- [28] J. Sanchez, F. Perronnin, T. Mensink, and J. Verbeek. Image classification with the fisher vector: Theory and practice. 2013. 4
- [29] R. G. Schneider and T. Tuytelaars. Sketch classification and classification-driven analysis using fisher vectors. *ACM Trans. Graph.*, 33(6):174:1–174:9, Nov. 2014. 2, 3, 6, 7
- [30] T. Shao, W. Xu, K. Yin, J. Wang, K. Zhou, and B. Guo. Discriminative sketch-based 3d model retrieval via robust shape matching. In *Computer Graphics Forum*, volume 30. Wiley Online Library, 2011. 8
- [31] K. Simonyan, A. Vedaldi, and A. Zisserman. Deep inside convolutional networks: Visualising image classification models and saliency maps. *CoRR*, abs/1312.6034, 2013. 6
- [32] K. Simonyan and A. Zisserman. Very deep convolutional networks for large-scale image recognition. *CoRR*, abs/1409.1556, 2014. 7
- [33] C. Szegedy, W. Liu, Y. Jia, P. Sermanet, S. Reed, D. Anguelov, D. Erhan, V. Vanhoucke, and A. Rabinovich. Going deeper with convolutions. *CoRR*, abs/1409.4842, 2014. 6
- [34] A. Vedaldi and B. Fulkerson. VLFeat: An open and portable library of computer vision algorithms. <http://www.vlfeat.org/>, 2008. 4
- [35] Z. Wu, S. Song, A. Khosla, F. Yu, L. Zhang, X. Tang, and J. Xiao. 3d shapenets: A deep representation for volumetric shape modeling. In *Proc. CVPR*, to appear, 2015. 1, 2, 3, 4, 5, 6
- [36] S. M. Yoon, M. Scherer, T. Schreck, and A. Kuijper. Sketch-based 3d model retrieval using diffusion tensor fields of suggestive contours. In *Proc. International Conference on Multimedia*, 2010. 8

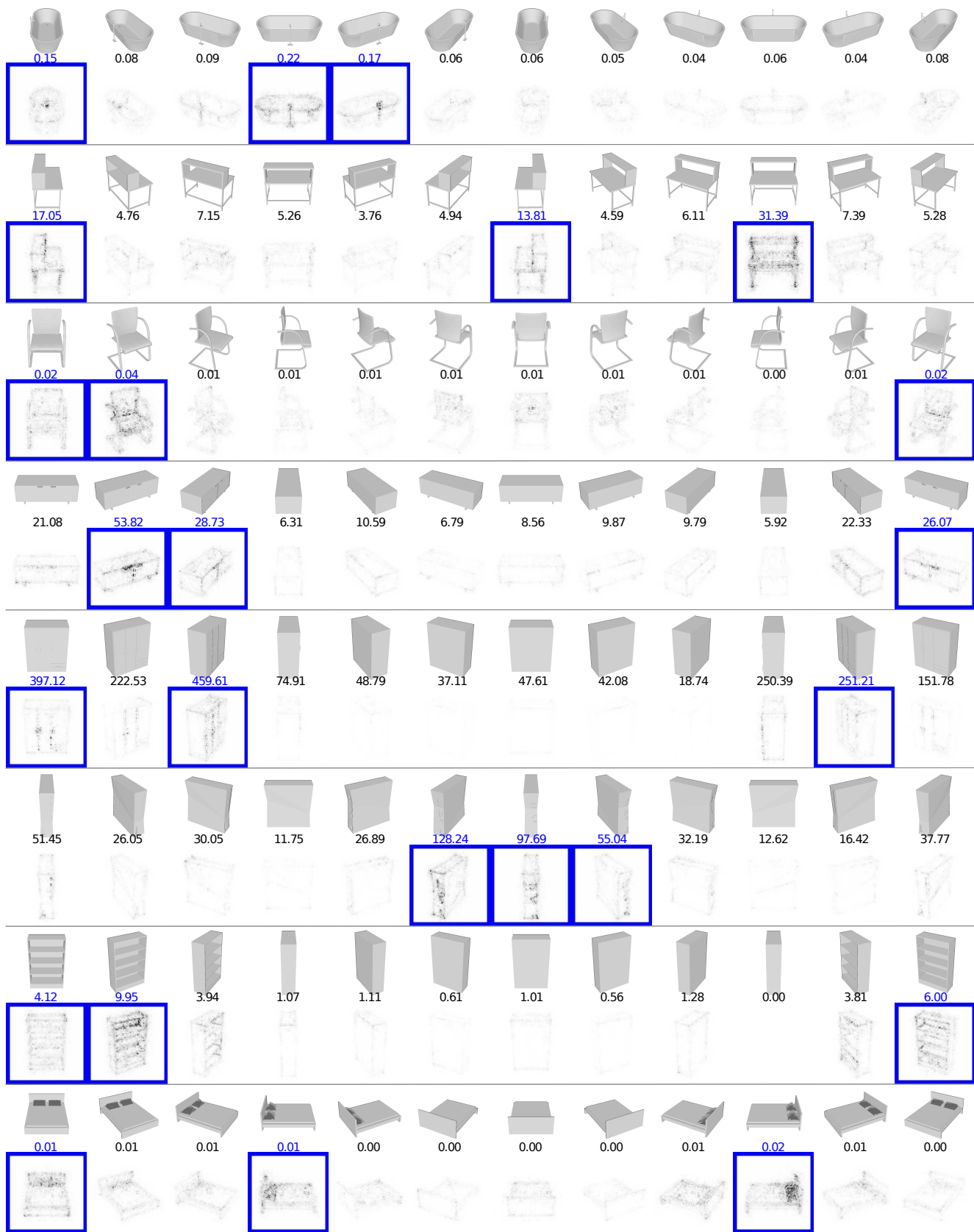


Figure 7. Additional examples of saliency maps. Top three views with the highest saliency are highlighted in blue and the relative magnitudes of gradient energy for each view is shown on top.



Figure 8. Examples of correctly and wrongly classified hand-drawn sketches. All sketches in each row are classified into the class labeled on top left. False positives are in red, with their ground truth classes labeled on top.